

# EUROPEAN ORGANIZATION FOR NUCLEAR RESEARCH

Proposal to the ISOLDE and Neutron Time-of-Flight Committee

## Coulomb Excitation and RDDS measurement of a Triaxial Superdeformed “ $\beta$ -band” in $^{162}\text{Yb}$

09 April 2024

R.A. Bark<sup>1</sup>, C. Fransen<sup>2</sup>, A.N. Andreyev<sup>3</sup>, N. Bernier<sup>4</sup>, M.G. Borge<sup>5</sup>, D. Bucher<sup>6</sup>, J.C. Cubiss<sup>3</sup>, F. Dunkel<sup>2</sup>, L. Gaffney<sup>7</sup>, J. Gerl<sup>8</sup>, K. Hadyńska-Klęk<sup>9</sup>, H. Hess<sup>2</sup>, R. Hirsch<sup>2</sup>, E. Ince<sup>9</sup>, M. Jafta<sup>4</sup>, J. Jolie<sup>2</sup>, P. Jones<sup>1</sup>, T. Kröll<sup>11</sup>, C.-D. Lakenbrink<sup>2</sup>, E. Lawrie<sup>1</sup>, J.J. Lawrie<sup>1</sup>, Z. P. Li<sup>12</sup>, S. Majola<sup>13</sup>, B.O. Mampaso<sup>5</sup>, C. Mehl<sup>4</sup>, S.M. Mullins<sup>14</sup>, C. Müller-Gatermann<sup>15</sup>, P.J. Napiorkowski<sup>9</sup>, C. Ngwetsheni<sup>4</sup>, S. Ntshangase<sup>16</sup>, G. O’Neill, N. Orce<sup>4</sup>, C. Page<sup>3</sup>, J. Pakarinen<sup>17</sup>, N. Pietralla<sup>11</sup>, L. Pellegri<sup>1</sup>, P. Reiter<sup>2</sup>, A. Ilana<sup>18</sup>, J. Srebrny<sup>9</sup>, M. Stryczyk<sup>17</sup>, J.F. Sharpey-Schafer<sup>16</sup>, F. von Spee<sup>2</sup>, N. Warr<sup>2</sup>, K. Wrzosek-Lipska<sup>9</sup>, M. Wiedeking<sup>1</sup>, Z. Yue<sup>3</sup> and S.Q. Zhang<sup>19</sup>

<sup>1</sup> *iThemba Laboratory for Accelerator Based Sciences, Cape Town, South Africa*

<sup>2</sup> *Institut für Kernphysik, Universität zu Köln, Zùlpicher Straße 77, D-50937 Köln, Germany*

<sup>3</sup> *University of York, United Kingdom*

<sup>4</sup> *Department of Physics and astronomy, University of the Western Cape, Belville, South Africa*

<sup>5</sup> *ISOLDE, CERN*

<sup>6</sup> *University of Cape Town, Cape Town, South Africa*

<sup>7</sup> *University of Liverpool, United Kingdom*

<sup>8</sup> *GSI, Helmholtzzentrum für Schwerionenforschung GmbH, Darmstadt, Germany*

<sup>9</sup> *Heavy Ion Laboratory, University of Warsaw, Poland*

<sup>10</sup> *Istanbul University-Cerrahpasa Hasan Ali Yucel Education Faculty, Department of Science Education, Büyükçekmece, Istanbul, Turkey.*

<sup>11</sup> *Institut für Kernphysik Technische Universität Darmstadt, Germany*

<sup>12</sup> *School of Physical Science and Technology, Southwest University, Chongqing, 400715, China*

<sup>13</sup> *University of Johannesburg, Johannesburg, South Africa*

<sup>14</sup> *Botswana International University of Science and Technology, Botswana*

<sup>15</sup> *Argonne National Laboratory, 9700 S Cass Ave, Lemont, IL 60439, United States*

<sup>16</sup> *University of Zululand, Richards Bay, South Africa*

<sup>17</sup> *University of Jyväskylä, Department of Physics, Jyväskylä, Finland*

<sup>18</sup> *Grupo de Física Nuclear & IPARCOS, Universidad Complutense de Madrid, Madrid, Spain*

<sup>19</sup> *Key Laboratory of Nuclear Physics and Technology, School of Physics, Peking University, Beijing 100871, China*



### Abstract

Relativistic Mean Field calculations predict that the  $0_2^+$  bands of Er and Yb isotopes around N=90 and 92 have a deformation of  $\beta_2 \sim 0.45$  and  $\gamma \sim 10^\circ$ . This is a rather fascinating prospect since the  $0_2^+$  bands, which are nominally  $\beta$ -vibrational bands, will have a similar deformation to bands at high-spin in this region, which have been identified as “triaxial superdeformed bands”. The calculations are supported by the large observed moments-of-inertia of the “ $\beta$ -bands” in these nuclei. Coulomb excitation measurements combined with lifetime measurements using the Recoil Distance Doppler-Shift technique (RDDS) are proposed to give a measure of the deformation of these bands, including the triaxiality parameter  $\gamma$ . This proposal is a follow-on from Letter of Intent 226, which asked for the development of  $^{160,162,164}\text{Yb}$  beams, to check the maximum achievable intensities, and beam contaminants, for Coulomb excitation and plunger measurements of the “ $\beta$ -bands”.

**Requested shifts:** 24 shifts

**Beamline:** Miniball, IDS

### Scientific Motivation

For many years, the  $0_2^+$  (or  $0_\beta^+$ ) bands of well-deformed nuclei were understood as “ $\beta$ -vibrations” following the seminal works of Bohr and Mottelson [Bo52, Bo53]. Nevertheless, it became clear that low-lying  $0^+$  bands could also arise due to other effects such as e.g. shape-coexistence [He11], and quadrupole pairing [Sh19]. Even the very existence of  $\beta$ -bands has been questioned some years ago [Ga01]. In nuclei with  $R_{4/2} = E(4_1^+)/E(2_1^+) = 2.91$ , such as those in the vicinity of N=90, there is also the opportunity to manifest the critical point symmetry X(5) [Ia01]. Here, we wish to explore the possibility that in the light Yb isotopes, in the N=90 region, the “ $\beta$ -band” could actually have a triaxial superdeformed (TSD) shape.

The proposal is motivated by our recent experimental results and calculations around N=90 [Ma19]. In Fig.1, the level energies of the so-called  $\beta$ - and  $\gamma$ -bands for the N=90, 92 nuclei  $^{156}\text{Dy}$  and  $^{160,162}\text{Yb}$  are presented, where the energies of a rigid rotor have been subtracted. The data are compared to calculations based on potential energy surfaces (PES's) calculated with the Relativistic Mean Field (RMF) and a 5-dimensional collective Hamiltonian (a modern version of the Bohr-Hamiltonian).

In both the experiment and theory, there is a striking difference in behavior of the  $0_2^+$  bands between  $^{156}\text{Dy}$  and  $^{160}\text{Yb}$ . In the former, the  $0_2^+$  band runs parallel to both the ground and  $\gamma$ -bands, while in the latter, the  $0_2^+$  band crosses the  $\gamma$ -band, as they have a larger moment-of-inertia than either the ground or  $\gamma$ -bands. Like  $^{160}\text{Yb}$ , the  $0_2^+$  band of  $^{162}\text{Yb}$  has a much higher moment-of-inertia than the ground band. These features can be explained by the RMF PES's (RMF+BCS with PC-PK1 density functional [Ma19]) shown in Fig. 2. In  $^{156,158}\text{Dy}$ , a single prolate minimum is calculated near  $\beta=0.3$ , and as a result, two  $\beta$ -vibrational bands are predicted. The  $0_2^+$  and  $0_3^+$  bands are spaced equally to the spacing between ground band and  $0_2^+$  bands, as expected for a first and second  $\beta$ -vibrational band. However, in  $^{160,162}\text{Yb}$ , a second, triaxial, highly-deformed minimum is visible in the PES at  $(\beta,\gamma) \sim (0.45,10^\circ)$  which is absent in the surfaces of the Dy isotopes. So, in the model, the  $0_2^+$  bands of  $^{160,162}\text{Yb}$  are shape-coexisting TSD bands, while the  $0_3^+$  band is the band based on the first  $\beta$ -phonon. (These bands mix strongly below spin 4 in the calculations for  $^{160}\text{Yb}$ ). Interestingly, these TSD “ $\beta$ -bands” are predicted in a region where TSD bands have been reported at *high spin* e.g. in Lu isotopes [Sc95, Ød01] and in  $^{160}\text{Yb}$  itself [Ag08]. Although lifetimes have been measured in the ground band in even-even nuclei in this region [e.g. Fe88, Mc06], the higher-spin members of the  $\beta$ - and  $\gamma$ -bands in the Yb isotopes have only recently been discovered, following measurements at iThemba LABS [Ma19, Md18]. No data

on level lifetimes of yrare low-spin states and transition strengths from such states are known so far for the nuclei of interest, which hampers a clear interpretation of the structure of the  $\beta$ -bands and motivates this work.

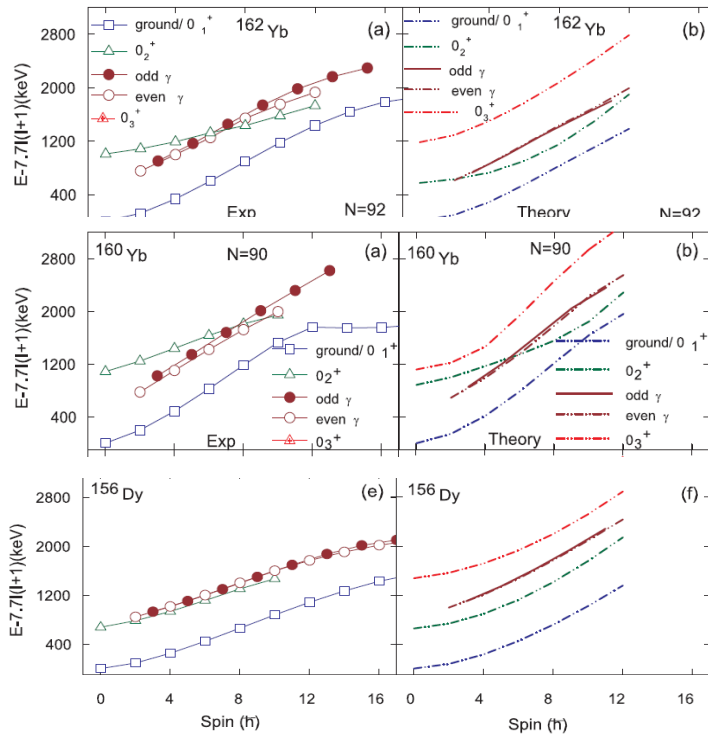


Figure 1. Experimental ground,  $\beta$ - and  $\gamma$ -bands (left) compared with calculation (right) [Ma19].

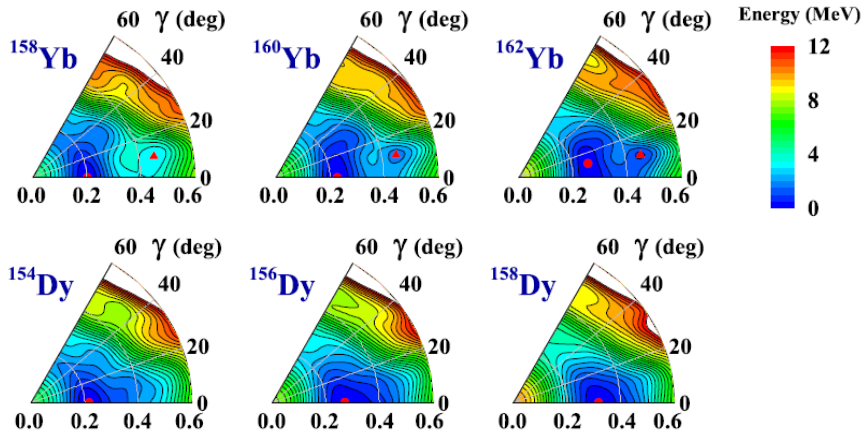
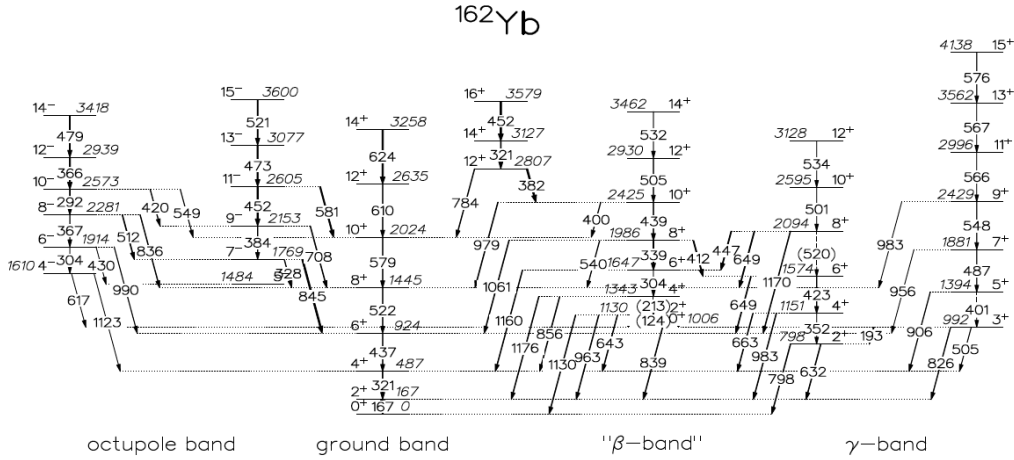


Figure 2. PES's of  $N=88$ ,  $N=90$  and  $N=92$  Dy and Yb isotones in the  $\beta$ - $\gamma$ -plane. Minima are marked with red symbols, circles and triangles represent the global and secondary minima, respectively. The energy spacing in the contour lines is 0.25 MeV [Ma19]. RMF PES around  $N=90$  [Ma19].

## Experiments

In our Letter of Intent (LOI226), two methods were proposed to obtain transition rates related to the “ $\beta$ ”-band – an RDDS plunger measurement and Coulomb Excitation. Time was granted to test the yields and purity of  $^{160,162,164}\text{Yb}$  beams; the  $^{160}\text{Yb}$  beam was found to have high (50%) contamination while  $^{162}\text{Yb}$  and  $^{164}\text{Yb}$  had yields of over  $10^9$  pps/ $\mu\text{C}$  with 10% and 5% contamination, respectively. Since the “ $\beta$ ”-band of  $^{164}\text{Yb}$  is not confirmed above spin 2 [Si18], we have chosen to measure transition rates in  $^{162}\text{Yb}$ , where the band members and their decay branching ratios are better understood (see

Fig. 3). With an upper limit of  $2 \times 10^8$  particles for charge breeding, and a 2.3% transport efficiency to Miniball, up to  $5 \times 10^6$  pps can be expected on target. While much is known about the level scheme of  $^{162}\text{Yb}$  [Mc04, Md18], the  $4_{\beta} \rightarrow 2_{\beta}$  and  $2_{\beta} \rightarrow 0_{\beta}$   $\gamma$ -ray transitions have not been reported. We also propose to search for these transitions using the IDS.



**Figure 3.** Low-lying levels of  $^{162}\text{Yb}$ , from the in-beam work of [Md18] and the decay work of [Mc04], including the ground, “ $\beta$ ”,  $\gamma$ -bands and octupole vibrational bands. Transitions in parenthesis have not been observed.

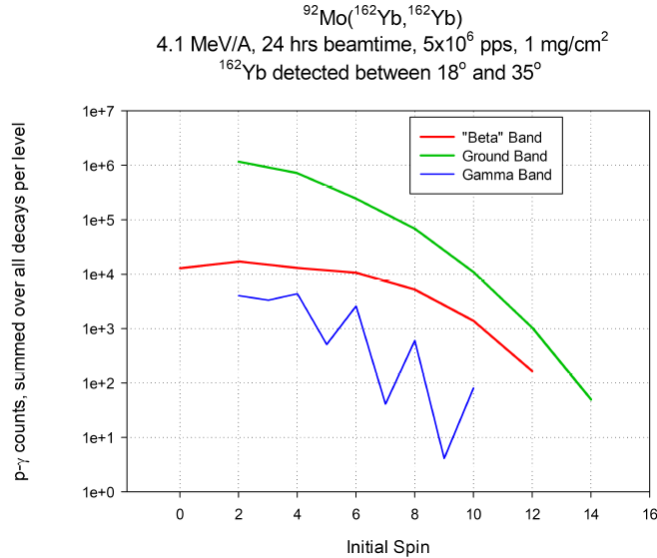


**Figure 4.** Integrated  $p$ - $\gamma$  coincidence counts of a safe Coulomb Excitation measurement for the levels of the ground,  $0_2^+$  and  $\gamma$ -bands of  $^{162}\text{Yb}$ . The detected particle is  $^{162}\text{Yb}$ .

## Coulomb Excitation

Transition matrix elements will be measured so that the quadrupole moment and the triaxiality parameter  $\gamma$  can then be deduced using Kumar-Cline sum rules [Cl86]. In Fig. 4, integrated  $p$ - $\gamma$  yields for the  $^{92}\text{Mo}(^{162}\text{Yb}, ^{162}\text{Yb})$  reaction, as a function of spin, have been calculated using GOSIA, with the QQQ2 charged particle detector array (CD detector) subtending the forward angles between  $18^\circ$  and  $35^\circ$ , and assuming an energy-independent 7%  $\gamma$ -ray detection efficiency for the Miniball array. Matrix elements were derived from known lifetimes for the ground band [Mc06], and calculated [Ma19]  $B(E2)$  values for the  $0_2^+$  and  $\gamma$ -band. The calculated daily  $p$ - $\gamma$  counts for members of the  $0_2^+$  band, (summed over all  $\gamma$ -decays per level), obtained for a beam of  $5 \times 10^6$  pps on a  $1 \text{ mg/cm}^2$   $^{92}\text{Mo}$  target, are over  $10^4$  counts per level up to the  $6_2^+$  state. The calculated and experimental branching ratios differ for decays from the  $\beta$ -band, so in Table 1, *experimental* branching ratios [Md18, Re07] are used

to estimate p- $\gamma$  yields for individual transitions depopulating the  $0_2^+$  band. Note that the levels in the  $0_2^+$  band typically decay via a strong transition of energy around 1 MeV.

The effect of Doppler broadening on the lineshapes has been estimated by using the opening angle of the Miniball detector segments for the detector width, and adding an intrinsic resolution of 2.3 keV in quadrature. For a 1 MeV  $\gamma$ -ray, the FWHM ranges from 4 keV to 16 keV, with a typical resolution of 12 keV. With these values in hand, we have checked the decays from each level to see if any peaks would overlap. The cleanest lines for each level are those highlighted in yellow. The intensities of other transitions depopulating a level can then be obtained knowing the branching ratios. The only (small) concern is the proximity of the 1160 and 1176 keV lines, but the strength of the 1160 keV line can be derived from the branching ratio and the strength of the 304 keV line.

**Table 1. Estimated  $\gamma$ -ray yields, assuming constant efficiency (7%) and 1 day of beam time, for transitions depopulating the  $\beta$ -band of  $^{162}\text{Yb}$ . “Clean” transitions are highlighted.**

		$^{162}\text{Yb}$		
Level	Transition	$E_\gamma$ (keV)	Experimental $\gamma$ -branching	p- $\gamma$ yield 1 mg/cm <sup>2</sup> $^{92}\text{Mo}$ $5 \times 10^6$ pps
$0_\beta$	$0_\beta \rightarrow 2_1$	839	100	13000
$2_\beta$	$2_\beta \rightarrow 0_1$	1130	100	7600
	$2_\beta \rightarrow 2_1$	963	74	5800
	$2_\beta \rightarrow 4_1$	643	50	4000
$4_\beta$	$4_\beta \rightarrow 2_1$	1176	100	12000
	$4_\beta \rightarrow 2_\beta$			
	$4_\beta \rightarrow 4_1$	856	8	960
$6_\beta$	$6_\beta \rightarrow 4_1$	1160	100	6360
	$6_\beta \rightarrow 4_\beta$	304	68	4320
	$6_\beta \rightarrow 6_1$			
$8_\beta$	$8_\beta \rightarrow 6_1$	1061	31	740
	$8_\beta \rightarrow 6_\beta$	339	44	1060
	$8_\beta \rightarrow 8_1$	540	44	1060
	$8_\beta \rightarrow 6_\gamma$	412	100	2400

## RDDS

The use of the  $^{92}\text{Mo}$  target produces inverse kinematics which allows the RDDS technique. Lifetimes of the lower states of the  $\beta$ -band will be measured and the data analyzed with the differential decay curve method [De12], which has many advantages [Ch17]. The Miniball detectors should be distributed over angles of approximately  $45^\circ$  and  $135^\circ$ . We propose to employ the Miniball plunger device for this experiment including the CD particle detector array mounted downstream from the plunger degrader to allow for a reconstruction of the kinematics, and thus an event-by-event Doppler correction of the  $\gamma$ -rays of interest. The latter is crucial to achieve a good separation of the Doppler-shifted components from  $\gamma$ -ray emission between target and degrader, and after the degrader, respectively, in spite of the rather large scattering angle of the  $^{162}\text{Yb}$  nuclei after the target, of up to  $35^\circ$ . The plunger device will be equipped with a 1.0 mg/cm<sup>2</sup>  $^{92}\text{Mo}$  self-supporting, stretched target and a  $^{\text{nat}}\text{Mg}$  degrader with a thickness of 2.5 mg/cm<sup>2</sup>. This target - degrader combination is the best compromise to achieve a large cross section for Coulomb excitation of  $^{162}\text{Yb}$  at the target and a predominant emission of the excited  $^{162}\text{Yb}$  nuclei at forward angles relevant for the detection with the CD detector and the RDDS measurement. Further, the  $^{\text{nat}}\text{Mg}$  degrader will lead to a low cross section for Coulomb excitation at the degrader (even though this contribution is not negligible and must be checked in the target-only run). In addition, the  $^{\text{nat}}\text{Mg}$  degrader will result in a small additional scattering of the  $^{162}\text{Yb}$  nuclei with an average angle of about  $5.8^\circ$ .

We would like to stress that recoiling  $^{92}\text{Mo}$  and  $^{24}\text{Mg}$  nuclei can be clearly discriminated from  $^{162}\text{Yb}$  with the CD detector. Kinematics calculations show that for angles smaller than  $33^\circ$  with respect to the beam axis, both energy and emission angle of  $^{162}\text{Yb}$  and  $^{92}\text{Mo}$  nuclei are sufficiently different to

distinguish the respective events using the high granularity of the CD detector in 16 rings and 96 radial stripes.

For the minimum observation angle of the CD detector of  $18^\circ$  with respect to the beam axis, the  $^{162}\text{Yb}$  nuclei have an energy after the target of  $E_T = 3.00$  MeV/A and are slowed down in the degrader to  $E_D = 1.61$  MeV/A. This corresponds to recoil velocities of  $v_T = 24.0$   $\mu\text{m}/\text{ps}$  and  $v_T/c = 0.080$  after target and  $v_D = 17.9$   $\mu\text{m}/\text{ps}$  and  $v_D/c = 0.060$  after the degrader. For the maximum usable scattering angle of  $^{162}\text{Yb}$  of  $33^\circ$ , the respective energies are  $E_T = 1.43$  MeV/A and  $E_D = 0.31$  MeV/A corresponding to  $v_T = 16.6$   $\mu\text{m}/\text{ps}$  and  $v_T/c = 0.0553$  after target and  $v_D = 7.7$   $\mu\text{m}/\text{ps}$  and  $v_D/c = 0.0258$  after the degrader.

The Doppler shifts and broadenings for these  $\gamma$ -rays, as a function of Miniball detector/CD-detector element angles have been calculated, and imply that degraded and undegraded components can be separated for about 30% of the detector combinations. The  $\gamma$ -rays from the  $0_\beta$ ,  $2_\beta$ , and  $4_\beta$  states, used for the RDDS measurement, of 839, 1130 and 1176 keV energy, will shift on to the 826 and 1160 keV lines. Nevertheless, by looking at either the forward or backward Miniball detectors one can isolate either the shifted or unshifted components from the contaminating lines, albeit at the expense of another factor of 2 in statistics. Taken together with the above restriction to 30% of detector combinations, the implication is that about 15% of the statistics listed in Table 1 will practically be available, or about 2000 counts per day for the 839 and 1176 keV lines and 1000 counts for the 1130 keV line.

As the lifetimes of interest, in the  $0_2^+$  bands, are all expected to be about a picosecond, based on the calculated matrix elements [MA19], only  $\sim 4$  target - degrader distances of a few to a few tens of micrometres are needed for this measurement. The detection of about 1000 counts per transition per distance should be sufficient to measure the lifetime to an accuracy of 10%.

*We propose to measure four distances for the RDDS measurement, with each distance to take a day. One day will be dedicated to a pure Coulomb Excitation measurement with the  $^{92}\text{Mo}$  target, with the degrader removed.*

## **$\beta$ -decay**

*This section is included for completeness. It has been considered for LoI 268, and awarded 2 shifts to test the intensity of the  $^{162}\text{Lu}$  beam.*

The  $\gamma$ -ray branching ratios for decays from the levels of the “ $\beta$ ”-band are necessary to determine the in-band  $B(E2)$  values. As the  $6^+$  and  $8^+$  levels show evidence of interactions at the crossing with the  $\gamma$ -band (see Figs. 1 and 2), the  $2^+$  and  $4^+$  levels become important, as they sample a “pure” superdeformed triaxial wavefunction. However, two important in-band transitions of the “ $\beta$ ”-band have not been reported so far. These are the 124 keV  $2^+ \rightarrow 0^+$  and the 213 keV  $4^+ \rightarrow 2^+$  transitions, (see Fig.6). This is undoubtedly due to the large  $(E_\gamma)^5$  factors in the expression for the transition rate, which favour out-of-band transitions. For example,  $(1130/124)^5 = 62847$ . In fact, using the  $B(E2)$  values of [Ma19] one may calculate the branching ratios  $P_\gamma(124)/\sum_i P_\gamma(i) = 5.3 \times 10^{-4}$  and  $P_\gamma(213)/\sum_i P_\gamma(i) = 10^{-2}$ , where  $P_\gamma(i)$  is the transition probability of the  $i$ th  $\gamma$ -ray depopulating the  $2^+$  or  $4^+$  level. However, the  $B(E2)$  values of [Ma19] predict that the 963 keV transition be only 3% of the intensity of the 1130 keV transition, while the experimental [Mc04] ratio is 74%. Because of this large discrepancy between theory and experiment, it is not possible to predict the 124 keV intensity with any reliability. In the best case scenario it could have a similar intensity to the 213 keV transition. Therefore we propose to measure at least the intensity of the 213 keV transition from the  $\beta$ -decay of  $^{162}\text{Lu}$ , which has a ground state with an 82s half-life, and isomers with 1.5 and 1.9 m half-lives, using the ISOLDE Decay Station (IDS). Two methods are considered, a singles measurement, or a coincidence measurement.

A clover singles spectrum of  $^{162}\text{Yb}$  from the decay of  $^{162}\text{Lu}$  is shown in Fig. 2(a) of [Mc04]. In this experiment,  $1.4 \times 10^{11}$  decays were presented to a clover array of 1.1% efficiency at 1.3 MeV. The relative intensities published by [Mc04], and singles spectrum allow a relation to be established

between the intensities and the counts seen in the spectrum. Taken together with the above branching ratio, the 213 keV transition would be expected to have around 900 counts in this spectrum, which would be swamped by the uncertainty on the background which is around 300000 counts high. To set the condition to observe a line in singles to e.g., 20% accuracy, we demand that the number of counts in the peak

$$N_{\gamma} > 5\sqrt{N_b}, \quad (1)$$

where  $N_b$  is the number of counts in the background. Assuming the IDS is equipped with 12 clovers, with an efficiency of 6% at 1.3 MeV, then this condition will be met if the overall decays presented to the detectors are increased by a factor of 6.2 for the 213 keV line, implying about  $8 \times 10^{11}$  decays would need to be presented to the IDS. Furthermore, to confirm that the 213 keV line belongs to  $^{162}\text{Yb}$ , its lifetime should be measured, which would require an out-of-beam measuring period of 3 half-lives. Alternatively, coincidences could be used.

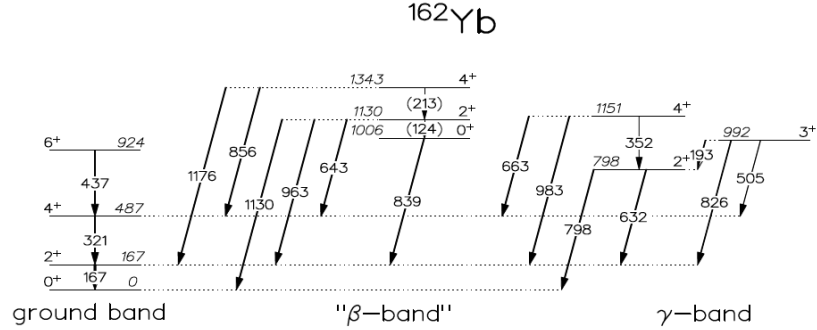


**Figure 5.** Close-up of the levels and related transitions of the ground, “ $\beta$ ” and  $\gamma$ -bands of  $^{162}\text{Yb}$ , as observed in  $\beta$ -decay [Mc04]. Transitions in parenthesis have not been observed.

#### Coincidences

In Fig. 2(b) of [Mc04] a coincidence gate on the 167 keV transition is presented. The background is reduced by a factor of about 250 compared to the singles spectrum. The peaks near 1.3 MeV are reduced by a factor 0.01 in this spectrum, due to requirement to detect the second  $\gamma$ -ray, resulting in an improvement in the peak-to-background ratio. In the IDS, peaks near 1.3 MeV would be expected to have a smaller reduction in height as the assumed efficiency is 0.06. To observe the 214 keV transition, we would gate on 1130, 963 and 643 lines which could be summed. (The 167 gate will probably be associated with a higher background but can also be used). A similar analysis now finds a factor of 22 increase in decays is required, or  $2.9 \times 10^{12}$  decays. The important point is that a shortened out-of-beam period is not required.

The listed intensity [ISLu] of the  $^{162}\text{Lu}$  beam, from a Ta target, is  $1.8 \times 10^7$  pps/ $\mu\text{C}$ . Ultimately, the amount of beam that can be utilized in the IDS clover array is limited by the counting rate in a detector. If the beam is continuously implanted into the tape, eventually the decay rate will equal the implantation rate, when  $t \gg \tau_{1/2}$ . With  $1.8 \times 10^7$  decays/second, and assuming each decay emits on average 2  $\gamma$ -rays, which are detected with 6% efficiency over 12 clovers,  $1.8 \times 10^5$  decays per detector are implied. However, in [Mc04], the  $1.4 \times 10^{11}$  decays only produced  $3.1 \times 10^8$  singles events. Allowing for the 1% efficiency of the Yale setup, it implies that only as much as 22% of the  $\beta$ -decays emitted  $\gamma$ -rays. Presumably the rest decayed to the ground state. Applying this final 22% correction to the IDS brings the rate per detector down to 40kHz. We propose to implant and count for 6 half-lives before moving the tape to limit the build-up of activity from the daughters. Under these conditions about  $10^{12}$  decays should be presented to the array per day. Three days of beamtime would allow the intensity of the 213 keV transition to be measured to an accuracy of about 20%. The 124 keV transition may be detected.

**Summary of requested shifts:** 15 shifts are requested for the coulex and RDDS of  $^{162}\text{Yb}$ . For the IDS measurement, we request 9 shifts of  $^{162}\text{Lu}$  beam.

## References:

- [Ag08] A. Aguillar et al., PR C **77**, 021302(R) (2008)
- [Bo52] A. Bohr, Mat. Fys. Medd. Dan. Vid. Selsk. **26**, 14 (1952).
- [Bo53] A. Bohr and B. R. Mottelson, Mat. Fys. Medd. Dan. Vid. Selsk. **27**, 16 (1953).
- [Ch17] A. Chester et al., Phys. Rev. C **96** 0211 (R) (2017)
- [Cl86] D. Cline Ann. Rev. Nucl. Part. Sci. **36** (1986) 683.
- [De12] A. Dewald et al. Prog. Part. Nucl. Phys. **67** (2012), 786
- [Fe88] M. P. Fewell et al., Phys. Rev. C **37**, 101 (1988).
- [Ga01] P.E. Garrett, J. Phys. G: Nucl. Part. Phys. **27**, R1 (2001).
- [He11] K. Heyde and J. L. Wood, Rev. Mod. Phys. **83**, 1467 (2011).
- [Ia01] F. Iachello, Phys. Rev. Lett. **87**, 052502 (2001)
- [ISLu] [http://isoyields-classic.web.cern.ch/lutetium\\_isotopes.html](http://isoyields-classic.web.cern.ch/lutetium_isotopes.html)
- [Ma19] S. Majola et al., Physical Review C **100**, 044324 (2019) and Z. Li, private communication.
- [Mc04] E.A. McCutchan *et al.* Physical Review C **69**, 024308 (2004)
- [Mc06] E.A. McCutchan *et al.* Physical Review C **73**, 034303 (2006)
- [Md18] L. Mdletshe Eur. Phys. J. A (2018) **54**: 176
- [Re07] C. W. Reich Nucl. Data Sheets **108**, 1807 (2007)
- [Sc95] H. Schnack-Petersen et al., Nucl.Phys. A **594** (1995) 175
- [Sh19] J.F. Sharpey-Schafer et al., European Physical Journal A (2019)55:15
- [Si18] Balraj Singh and Jun Chen, Nucl. Data Sheets **147**, 1 (2018)
- [Ød01] S. Ødegård et al., Phys. Rev. Lett. **86**, 5866 (2001).



# Appendix

## DESCRIPTION OF THE PROPOSED EXPERIMENT

The experimental setup comprises: *(name the fixed-ISOLDE installations, as well as flexible elements of the experiment)*

Part of the Choose an item.	Availability	Design and manufacturing
Beam Current Measurement after REX EBIS	<input checked="" type="checkbox"/> Existing	<input checked="" type="checkbox"/> To be used without any modification
Miniball + CD detector	<input checked="" type="checkbox"/> Existing	<input checked="" type="checkbox"/> To be used without any modification <input type="checkbox"/> To be modified
	<input type="checkbox"/> New	<input type="checkbox"/> Standard equipment supplied by a manufacturer <input type="checkbox"/> CERN/collaboration responsible for the design and/or manufacturing
IDS	X <input type="checkbox"/> Existing	X <input type="checkbox"/> To be used without any modification <input type="checkbox"/> To be modified
	<input type="checkbox"/> New	<input type="checkbox"/> Standard equipment supplied by a manufacturer <input type="checkbox"/> CERN/collaboration responsible for the design and/or manufacturing
[insert lines if needed]		

## HAZARDS GENERATED BY THE EXPERIMENT

*(if using fixed installation)* Hazards named in the document relevant for the fixed [MINIBALL + only CD, MINIBALL + T-REX] installation.

Additional hazards:

Hazards			
	[Part 1 of the experiment/equipment]	[Part 2 of the experiment/equipment]	[Part 3 of the experiment/equipment]
<b>Thermodynamic and fluidic</b>			
Pressure			
Vacuum	High Vacuum 10 <sup>-6</sup> mbar	High Vacuum 10 <sup>-6</sup> mbar	
Temperature	LN <sub>2</sub> 77 [K]	LN <sub>2</sub> 77 [K]	
Heat transfer			
Thermal properties of materials			
Cryogenic fluid	LN <sub>2</sub> , 1 Bar, 10l	LN <sub>2</sub> , 1 Bar, 10l	
<b>Electrical and electromagnetic</b>			
Electricity	[voltage] [V], [current][A]		
Static electricity			
Magnetic field	[magnetic field] [T]		
Batteries	<input type="checkbox"/>		
Capacitors	<input type="checkbox"/>		
<b>Ionizing radiation</b>			
Target material	[material]		
Beam particle type (e, p, ions, etc)	<sup>162</sup> Yb	<sup>162</sup> Lu	
Beam intensity	> 2 x 10 <sup>6</sup> pps	> 1.8 x10 <sup>7</sup> pps	
Beam energy	4.1 MeV/A		

Cooling liquids	[liquid]		
Gases	[gas]		
Calibration sources:	<input checked="" type="checkbox"/>		
• Open source	<input type="checkbox"/>		
• Sealed source	<input checked="" type="checkbox"/> [ISO standard]		
• Isotope	<sup>152</sup> Eu, <sup>133</sup> Ba, <sup>60</sup> Co	<sup>152</sup> Eu, <sup>133</sup> Ba, <sup>60</sup> Co	
• Activity	~ 10 kBq	~ 10 kBq	
Use of activated material:			
• Description	<input type="checkbox"/>		
• Dose rate on contact and in 10 cm distance	[dose][mSV]		
• Isotope			
• Activity			
<b>Non-ionizing radiation</b>			
Laser			
UV light			
Microwaves (300MHz-30 GHz)			
Radiofrequency (1-300MHz)			
<b>Chemical</b>			
Toxic	[chemical agent], [quantity]		
Harmful	[chemical agent], [quantity]		
CMR (carcinogens, mutagens and substances toxic to reproduction)	[chemical agent], [quantity]		
Corrosive	[chemical agent], [quantity]		
Irritant	[chemical agent], [quantity]		
Flammable	[chemical agent], [quantity]		
Oxidizing	[chemical agent], [quantity]		
Explosiveness	[chemical agent], [quantity]		
Asphyxiant	[chemical agent], [quantity]		
Dangerous for the environment	[chemical agent], [quantity]		
<b>Mechanical</b>			
Physical impact or mechanical energy (moving parts)	[location]		
Mechanical properties (Sharp, rough, slippery)	[location]		
Vibration	[location]		
Vehicles and Means of Transport	[location]		
<b>Noise</b>			
Frequency	[frequency],[Hz]		
Intensity			
<b>Physical</b>			
Confined spaces	[location]		
High workplaces	[location]		
Access to high workplaces	[location]		
Obstructions in passageways	[location]		
Manual handling	[location]		
Poor ergonomics	[location]		

### 0.1 Hazard identification

The longest lived activity from the  $^{162}\text{Lu}$  decay chains has a half-life of approximately 1 day.

3.2 Average electrical power requirements (excluding fixed ISOLDE-installation mentioned above): *(make a rough estimate of the total power consumption of the additional equipment used in the experiment)*

None above fixed ISOLDE-installation for beam development. Plunger uses < 1kW.